

Published in final edited form as:

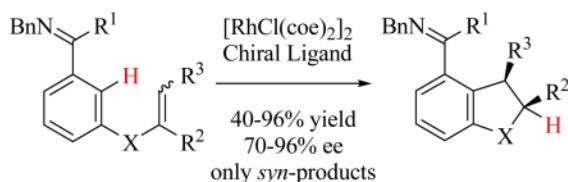
J Org Chem. 2008 September 5; 73(17): 6772–6779. doi:10.1021/jo801098z.

Enantioselective Intramolecular Hydroarylation of Alkenes via Directed C–H Bond Activation

 Hitoshi Harada, Reema K. Thalji, Robert G. Bergman^{*}, and Jonathan A. Ellman^{*}

Department of Chemistry, University of California, and Division of Chemical Sciences, Lawrence Berkeley National Laboratory, Berkeley, California 94720

Abstract



Highly enantioselective catalytic intramolecular ortho-alkylation of aromatic imines containing alkenyl groups tethered at the *meta* position relative to the imine directing group has been achieved using $[\text{RhCl}(\text{coe})_2]_2$ and chiral phosphoramidite ligands. Cyclization of substrates containing 1,1- and 1,2-disubstituted as well as trisubstituted alkenes were achieved with enantioselectivities >90% ee for each substrate class. Cyclization of substrates with *Z*-alkene isomers proceeded much more efficiently than substrates with *E*-alkene isomers. This further enabled the highly stereoselective intramolecular alkylation of certain substrates containing *Z/E*-alkene mixtures via a Rh-catalyzed alkene isomerization with preferential cyclization of the *Z*-isomer.

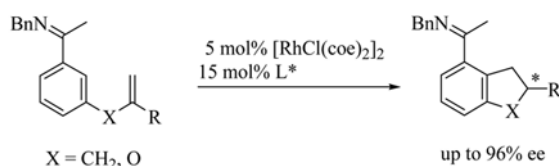
Introduction

Transition metal catalyzed carbon–hydrogen (C–H) bond activation¹ is one of the most powerful strategies for carbon–carbon (C–C) bond formation. Because the C–H bond is ubiquitous in organic substances, this method has broad potential. Moreover, direct conversion of C–H bonds into C–C bonds without intermediate pre-activation should shorten reaction sequences and reduce waste resulting in environmental benefits. Finally, catalytic C–H activation should enable novel bond connections to rapidly give rise to structurally complex molecules. In spite of these attractions, challenges in both the reactivity and selectivity for these transformations remain.

Following Murai's ground-breaking discovery of Ru-catalyzed chelation-assisted alkylation of aromatic ketones,² Jun reported that the scope of the reaction could be extended to isomerizable alkenes by the use of an imine directing group and Rh-catalyst.³ Previous work in our group extended this chemistry to intramolecular reactions, which showed significantly broadened reaction scope over intermolecular coupling reactions.⁴ For example, substrates with di- and even trisubstituted alkenes underwent cyclization, and aromatic aldimines and ketimines with heteroatom tethers such as vinyl ethers, allylic ethers, and allylic amines, also reacted cleanly. The synthetic utility of this transformation was demonstrated in its application to the synthesis of potent biologically active natural products and drug candidates.⁵

Examples of effective enantioselective catalytic C–H bond functionalizations are rare despite the high degree of activity in this area.⁶ Murai reported a chelation-assisted enantioselective alkylation utilizing the pyridine directing group in the intramolecular coupling of olefinic C–H bonds with alkenes; however, this transformation proceeds with only modest ee's.⁷ While the cyclization of the analogous imidazolyl-1,5-diene gave significantly higher enantioselectivities, the reaction is limited in generality.⁷ The atropselective alkylation of 2-arylpyridines by transition metal-catalyzed C–H functionalization has also been reported although the ee did not exceed 49%.⁸ More recently Widenhoefer has reported the enantioselective platinum-catalyzed intramolecular alkylation of indoles tethered to unactivated terminal alkenes with selectivities up to 90% ee.⁹ On the other hand, high stereoselectivity and broader substrate scope have been obtained in intramolecular hydroacylation as initially reported for the cyclization of 4-pentanal into β -substituted cyclopentanones.¹⁰ In addition, Yu has very recently also reported on the Pd-catalyzed enantioselective alkylation of diphenyl(2-pyridyl)methane with alkylboronic acids using monoprotected amino acids as the chiral ligands.¹¹

We previously communicated the catalytic enantioselective alkylation of aromatic ketimines with tethered 1,1-disubstituted alkenes (eq 1),¹² which represented one of the first highly enantioselective catalytic reactions involving aromatic C–H bond activation. Herein, we disclose the full details of this work and further report on ligand optimization that has enabled greatly expanded substrate scope, including the intramolecular hydroarylation of 1,2-disubstituted and 1,1,2-trisubstituted alkene substrates. Cyclization of substrates with *Z*-alkene isomers proceeded much more efficiently than substrates with *E*-alkene isomers. This further enabled the highly stereoselective intramolecular alkylation of certain substrates containing *Z/E*-alkene mixtures via a Rh-catalyzed alkene isomerization with preferential cyclization of the *Z*-isomer.



(1)

Results and Discussion

A. Enantioselective Cyclization of 1,1-Disubstituted Alkenes

A.1. Ligand Screening—We initiated our study by testing the cyclization of alkene **1** using Rh complexes with various ligands in order to identify the optimal ligand for this reaction. Our efforts focused on chiral monodentate ligands¹³ because catalysts derived from chelating phosphines were inefficient for this reaction.⁴ Of the range of chiral monodentate phosphines screened (Chart 1), only phosphoramidites gave acceptable enantioselectivities. A brief summary of results for chiral phosphoramidites and the structurally related TADDOL-based ligands is given in Table 1.

High enantioselectivities and complete conversions were obtained with the (*S*)-binol-derived phosphoramidites with a bulky amine substituent (**L9** – **11**, entries 11, 14, and 15). Alkene **1** cyclized quantitatively in the presence of 5 mol% [RhCl(coe)₂]₂ and 15 mol% **L10** to give **2** in 88% ee within 2 hours at 125 °C. In contrast, (–)-TADDOL-based phosphites **L1** – **3** (entries 1 – 3), (–)-TADDOL-based phosphonite **L4** (entry 4), (*S*)-binol-derived phosphites **L5** (entry 5), and phosphoramidites **L6** – **8** (entries 6 – 8) that incorporate unhindered secondary amines all proved to be ineffective catalysts, giving either poor conversions, poor ee's, or both. Both

diastereomeric ligands **L10** and **L11** afforded the same enantiomer in the same yield and with comparable enantioselectivities (entries 14 and 15). These data, combined with the result that **L9**, bearing an achiral amine substituent, also gave the same sense of induction (entry 11), indicates that the chirality of the binaphthyl moiety is primarily responsible for the asymmetric induction and that the sterics of the amine substituent, rather than its chirality, contribute to the overall induction and catalyst efficiency.

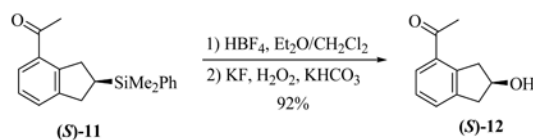
A.2. Further Optimization of Reaction Parameters—The ratio of ligand to Rh had a significant effect on the reaction efficiency. The optimal phosphoramidite to Rh ratio for the cyclization of **1** was found to be between 1:1 and 1.5:1. Increasing this ratio dramatically inhibited the reaction (Table 1, entries 9 – 13). Similar results have been observed in Rh-catalyzed hydrogenation using phosphoramidite ligands.¹⁴

To further enhance the enantioselectivity, the reaction temperature was lowered using ligands **L9**, **L10**, and **L11**, which all gave quantitative cyclizations of **1** at 125 °C (Table 1). Indeed, at 50 °C, **1** cyclized using **L10** in 95% ee and 94% yield in only 9 hours (Table 2, entry 2). Increases in enantioselectivities were also obtained using ligands **L9** and **L11** at lower temperatures, although the reactions were significantly slower (Table 2, entries 1 and 3).

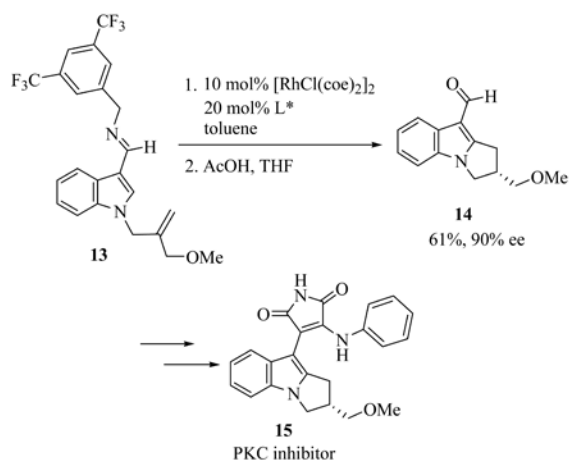
A.3. Substrate Scope—To explore the scope of this enantioselective cyclization, substrates **3**, **5**, **7**, and **9** were evaluated using the optimal ligands **L9**, **L10**, and **L11** (Table 2). These substrates cyclized in nearly quantitative yields under the optimal conditions for each substrate. Ligands **L10** and **L11** consistently gave faster reaction rates than **L9**. Ligands **L10** and **L11** also showed higher enantioselectivities for all substrates except the sterically encumbered silyl substrate **3**, for which the least hindered ligand **L9** gave the optimal result (70% ee, entry 4).

Vinyl ether **9** exhibited the most efficient reaction of all the substrates explored. Even at room temperature the reaction proceeded cleanly with ligand **L10** giving the desired product (**R**)-**10** in high yield and with 96% ee (entry 16). Ligand **L11** afforded a less efficient catalyst but provided the same high level of selectivity as that obtained with diastereomer **L10** (entry 18).

A4. Applications of Enantioselective Cyclizations of 1,1-Disubstituted Alkene Substrates—The substrate examples shown above demonstrate the utility of this methodology for the synthesis of a diversity of chiral products including chiral indanes, dihydropyrroloindoles, and dihydrobenzofurans. In addition, the cyclization of alkene **3** enables the introduction of a hydroxyl group, as the SiMe₂Ph functionality can be oxidized with retention of configuration using the conditions developed by Fleming¹⁵ and Tamao.¹⁶ Phenylsilane (**S**)-**11** was converted to the fluorosilane, which was cleanly oxidized using mild hydrogen peroxide conditions to give (**S**)-**12** in 92% overall yield (eq. 2).¹² Furthermore, we also applied the enantioselective cyclization methodology to the asymmetric synthesis of the potent protein kinase C inhibitor tricyclic indole **15** (eq. 3).^{5b} In the course of the synthesis, a key intermediate **14** was prepared in 61% yield and 90% ee by the cyclization of alkene **13**. This synthesis is noteworthy not only because it provided much more efficient entry to inhibitor **15**, but also because it represents the first example of the enantioselective catalytic cyclization of an aldimine rather than a ketimine substrate.



(2)



(3)

B. Enantioselective Cyclization of 1,2-Disubstituted Alkenes

Next, our study focused on 1,2-disubstituted alkenes, which were more difficult substrates for enantioselective cyclization because *Z/E*-alkenes isomerization occurs at rates that are competitive with cyclization.

B.1. Initial Evaluation of Olefin Isomers—We began our study on 1,2-disubstituted alkene substrates by examining which of three isomeric alkenes, **16**, **17**, and **18**, provided the 2,3-dihydro-3-methylbenzofuran product **19** with the greatest efficiency and selectivity (Table 3). We also monitored alkene isomerization as the reactions proceeded. *Z*-Alkene **18** was the best substrate with respect to both yield and enantioselectivity (entry 3). Alkene **18** cyclized in the presence of 10 mol% [RhCl(coe)₂]₂ and 20 mol% **L10** to give (*R*)-**19** in 82% yield and 85% ee in 96 hours at 50 °C. None of the benzopyran that might be produced upon isomerization of the alkenyl group from vinyl to allyl was seen. Much lower yield and enantioselectivity were observed in the reaction of allyl substrate **16** (entry 1). Reaction of *E*-alkene **17** was slower than that of the *Z*-isomer **18** (entry 2). However, both isomers gave the same stereoselectivity, and *Z/E* isomerization of the substrate was observed during the cyclizations of both **17** and **18** (entries 2 and 3). It is therefore likely that regardless of the *Z* or *E* stereochemistry of the starting material, cyclization proceeded through the *Z*-alkene.

B.2. Ligand Screening—We next screened various phosphoramidite ligands (Chart 1)¹³ for enhancing the enantioselectivity of the reaction using *Z*-alkene **18** as a substrate (Table 4). *N,N*-Diisopropylphosphoramidite **L9** provided high yield and the highest enantioselectivity among the (*S*)-binaphthyl type of ligands (76% yield, 87% ee, entry 2). *N,N*-Dicyclohexylphosphoramidite **L12** showed lower selectivity (77% ee, entry 5) compared to **L9**. Increased steric hindrance as exemplified by the *N-tert*-butyl, *N*-isopropylphosphoramidite **L13** (entry 6) resulted in a dramatic decrease in yield as did the less hindered *N,N*-dibenzylphosphoramidite **L8** (entry 1). Ligand **L11**, the diastereomer of **L10**, provided lower yield but the same stereoselectivity as **L9** and **L10** (61% yield, 85% ee, entry 4). These results indicate that the stereoselectivity is predominantly controlled by the diol moiety of the phosphoramidite ligands, in analogy to what was observed in the reaction of 1,1-disubstituted alkenes. Accordingly, the chiral diol was varied, keeping the diisopropylamino group intact. (*S*)-Octahydrobinaphthol-based ligand **L18** gave the best result (82% yield and 91% ee, entry 11). (*S*)-Dimethylbinaphthol-based ligand **L14** also resulted in increases in enantioselectivity (90% ee, entry 7), and the (*S*)-VANOL-based ligand **L16** (entry 9) and the (*S*)-VAPOL-based ligand **L17** (entry 10) accelerated the cyclization; however, none of these were better than **L18** overall. The hindered (*S*)-biphenol-, (*S*)-octahydrobinaphthol-, and (–)-TADDOL-based

ligands, **L15** (entry 8), **L20** (entry 13), and **L21** (entry 14), respectively, all gave dramatically reduced yields.

B.3. Further Optimization of Reaction Parameters—In the interest of exploring reaction efficiency, we further investigated the reaction conditions using **18** as a substrate and **L18** as a ligand (Table 5). Increasing the temperature from 50 to 75 °C accelerated the reaction and resulted in only a modest reduction in selectivity (entry 2). Although high enantioselectivities were obtained in all solvents that were investigated (entries 1, 3, and 4), 1,4-dioxane provided both the fastest reaction and the highest conversion (entry 4).

B.4. Substrate Scope—We also studied the scope of 1,2-disubstituted alkenes in this enantioselective cyclization reaction using the optimal ligands (Table 6). The ethyl-, *i*-butyl-, and phenyl-substituted substrates **20**, **22**, and **24** all cyclized with high enantioselectivities (entries 2–4). In the reactions of aldimine substrate **26**, enantioselectivities were high, but the yields were much lower than for the corresponding ketimine substrate **18** regardless of ligand used (entries 5–7). In addition, **L19** rather than **L18** provided the highest enantioselectivity for the cyclization of aldimine substrate **26** (87–89% ee, entry 7).

C. Stereoselective Cyclization of 1,1,2-Trisubstituted Alkenes

Finally, we explored the challenging stereoselective cyclization of 1,1,2-trisubstituted alkenes, in which two stereocenters would be set. We began our investigation with olefin isomers **28** and **29**. We again monitored not only conversion to product but also alkene isomerization (Table 7). Reaction of the *E*-alkene isomer **28** using **L16** in toluene at 75 °C for 68 hours gave **30** in modest yield and with low enantioselectivity (40% yield and 31% ee, entry 1). In contrast, a faster reaction that resulted in a higher yield and enantioselectivity was observed for substrate **29**, which was a 4:1 mixture of *Z* and *E* isomers (81% yield and 69% ee, entry 2). The enantioselectivity of the reaction was increased by lowering the reaction temperature and by using 1,4-dioxane as the solvent (80% ee, entry 3). Ligands **L18** and **L19** resulted in additional increases in enantioselectivity, although the reaction efficiency was lower than that observed for **L16** (entries 4 and 5). The highest selectivity was achieved with **L19** (91% ee, entry 5), and with this ligand, the *E*-isomer **28** was completely unreactive to either cyclization or alkene isomerization. Additionally, trisubstituted alkene substrate **31** also cyclized to yield (**2S**, **3R**)-**32** with high enantioselectivity, although a higher reaction temperature was required in this case (Table 6, entry 9). Interestingly, cyclization of the 1,1,2-trisubstituted alkene substrates **29** and **31**, which were *Z/E* mixtures, gave only the *syn*-isomer products as determined by NMR and X-ray structural analysis (see Supporting Information and Section D), further indicating that when *Z/E* mixtures of trisubstituted alkene substrates are used only the *Z*-alkene isomer, which is expected to give the *syn*-product, cyclizes.

D. Determination of Absolute Configuration for Cyclization Products

The absolute configuration of the two cyclization products, (**R**)-**19** and (**2R,3R**)-**30**, were determined by X-ray crystallography after their derivatization. The *N*-benzylimine (**R**)-**19** was hydrolyzed under acidic conditions and the resulting ketone was converted to the *N*-sulfinyl imine (**S_S**,**R**)-**33** by condensation with (*S*)-2,4,6-trimethylbenzenesulfinamide (Figure 1). (**2R,3R**)-**30** was similarly derivatized to hydrazone (**2R,3R**)-**34** (Figure 2). CIF files for the X-ray crystal structures of (**S_S**,**R**)-**33** and (**2R,3R**)-**34** are provided in the Supporting Information. The absolute stereochemistry of the representative cyclized products was thus determined to be (**R**)-**19** and (**2R,3R**)-**30**. The absolute configurations of (**R**)-**21**, (**R**)-**23**, (**R**)-**25**, (**R**)-**27**, and (**2S,3R**)-**32** were assigned by analogy to the absolute configurations of (**R**)-**19** and (**2R,3R**)-**30**.

E. Mechanistic Discussion

Phosphoramidites have recently gained prominence as ligands for asymmetric catalysis due to their remarkable effects in catalytic asymmetric conjugate additions¹⁷ and Rh-catalyzed hydrogenation reactions.¹⁴ The exceptional rates and stereoselectivities observed may be attributed to the unique binding properties of the phosphoramidite ligands, which include σ donation to the metal center and enhanced π acceptor ability compared to phosphines.

The results presented in Table 1 (entries 9 – 13), which display the effect of the ligand-to-Rh ratio, strongly suggest that only one ligand is bound to one Rh center throughout the catalytic cycle. Excess ligand most likely generates an inactive Rh species having more than one phosphoramidite ligand bound. This conclusion is also supported by the fact that phosphoramidites bind very strongly to Rh as a result of their π acceptor properties.¹⁴ Thus, it seems likely that multiple phosphoramidite ligands on a Rh center could render it inactive.

Based on our results, and in accordance with the catalytic cycle described by Jun¹⁸ for the analogous intermolecular reaction, a possible catalytic cycle is given in Scheme 1. Pre-coordination of the imine and successive C–H oxidative addition to the Rh center would generate a Rh–H complex **35**. Coordination of the alkenyl group to the metal, followed by migratory insertion of the double bond into the Rh–H bond, would provide metallacycle **36**, which can then undergo reductive elimination to afford the product. Deuterium labeling studies performed by Jun and coworkers on the analogous intermolecular reaction indicate that the reductive elimination step is rate-determining.¹⁸

The stereoselectivities are presumably due to highly diastereoselective migratory insertion. The fact that both *Z*- and *E*-isomers of 1,2-disubstituted alkenes give the same selectivity (Table 3, entries 2 and 3) can be rationalized by the observation that the *E*-olefin isomer was converted to the *Z*-isomer during the reaction, which could then react. The trisubstituted *E*-alkene substrate **28** reacted much more slowly and with lower selectivity than that of the corresponding substrate **29** with a 4:1 *Z*- to *E*-isomer ratio (Table 7, entries 1 and 2). This lower selectivity can perhaps be explained by isomerization of the double bond from vinyl to allyl, which then cyclized with decreased selectivity, similar to that observed in the reaction of **16** (Table 3, entry 1).

Conclusions

In summary, we have developed a highly stereoselective intramolecular hydroarylation of alkenes via directed C–H bond activation using a Rh/chiral phosphoramidite catalyst system, which represents a very rare example of an enantioselective catalytic reaction involving aromatic C–H bond activation.

Moreover, the identified catalyst system enables the intramolecular alkylation reaction to proceed at low temperatures, leading to increased selectivity. Finally, good substrate scope was achieved with 1,1- and 1,2-disubstituted as well as 1,1,2-trisubstituted alkenes all serving as effective substrates. For the cyclization of the 1,2-disubstituted and 1,1,2-trisubstituted alkenes, the *Z*-alkene isomers were much more effective substrates than the corresponding *E*-isomers. This stereoselective catalytic transformation provides access to a range of chiral indanes, dihydrobenzofurans, and dihydropyrroloindoles with different substitution patterns and therefore should be applicable to the asymmetric synthesis of a range of biologically active compounds.

Experimental Section

General procedure for ¹H NMR experiments

In a glovebox, to a medium-walled NMR tube was added a mixture of [RhCl(coe)₂]₂ (0.005 mmol, 10 mol%), phosphoramidite ligand (0.010 mmol, 20 mol%) in 0.40 mL of solvent, and a solution of imine (0.050 mmol) and 2,6-dimethoxytoluene internal standard (0.010 mmol) in 0.10 mL of solvent. The tube was fitted with a Cajon adapter, the mixture was frozen using liquid N₂, and then the tube was flame sealed under vacuum. The NMR tube was then placed in oil bath heated to the appropriate temperature and the progress of the reaction was monitored periodically by ¹H NMR spectroscopy. After the indicated reaction time, the sealed tube was opened and the mixture was concentrated. The residue was dissolved in a small amount of methylene chloride, silica gel was added, and the mixture was concentrated to dryness. The residue was subjected to silica gel column chromatography and eluted with a 1:20 mixture of ethyl acetate and hexanes for chiral HPLC analysis. Racemates for HPLC analysis were prepared as crude material by using PCy₃ or FcPCy₂ as a ligand instead of a chiral phosphoramidite.

(*R*)-1-(3-Methyl-2,3-dihydrobenzofuran-4-yl)ethanone ((*R*)-48) [Table 6, entry 1]

In a glovebox, to a medium-walled NMR tube was added a mixture of [RhCl(coe)₂]₂ (3.6 mg, 0.0050 mmol) and (*S*)-diisopropyl-(8,9,10,11,12,13,14,15-octahydro-3,5-dioxo-4-phosphacyclohepta[2,1-*a*;3,4-*a'*]dinaphthalen-4-yl)amine (4.2 mg, 0.0099 mmol) in 1,4-dioxane (0.40 mL) and a solution of benzyl-[1-{3-[(*Z*)-propenyl]oxy}phenyl]ethylidene]amine (13.4 mg, 0.0505 mmol) in 1,4-dioxane (0.10 mL). The tube was fitted with a Cajon adapter, the mixture was frozen, and then the tube was flame sealed under vacuum. The NMR tube was then placed in oil bath heated to 50 °C for 48 h. After the reaction, the sealed tube was opened and the mixture was concentrated. To the residue were added 1,4-dioxane (0.50 mL) and concentrated HCl/H₂O (1/1) (0.50 mL). The mixture was stirred at room temperature for 3 h and then extracted with diethyl ether four times. The combined organic layer was concentrated and the residue was purified by silica gel column chromatography (silica gel: 15 mL, eluted with 20:1 hexanes/ethyl acetate) to give the title compound as a colorless oil (6.3 mg, 71% yield). IR (ZnSe, thin film) ν_{\max} (cm⁻¹): 1680, 1584, 1442, 1355, 1256, 1236. ¹H NMR (400 MHz, CDCl₃): δ 7.38 (d, *J* = 8.0 Hz, 1H), 7.23 (t, *J* = 8.0 Hz, 1H), 6.99 (d, *J* = 8.0 Hz, 1H), 4.54 (t, *J* = 8.6 Hz, 1H), 4.29 (dd, *J* = 2.8, 8.6 Hz, 1H), 4.04–3.96 (m, 1H), 2.60 (s, 3H), 1.24 (d, *J* = 6.8 Hz, 3H). ¹³C{¹H} NMR (100 MHz, CDCl₃): δ 199.0, 160.5, 133.8, 133.6, 128.2, 122.1, 114.1, 79.0, 37.0, 28.1, 20.1. HRMS (EI): *m/z* calcd. for C₁₁H₁₂O₂ (M⁺): 176.08373; found: 176.08366. Chiral HPLC (Chiralcel AS column, 1% *i*PrOH/hexanes, 1mL/min): major, 6.41 min; minor, 5.90 min; 90% ee. [α]_D²⁵ +135.35 (c 0.99, CHCl₃). Maximum value based upon sample enantiomeric purity: [α]_D²⁵ +150.39 (c 0.99, CHCl₃).

By a similar procedure starting from benzyl-[1-{3-[(*Z*)-propenyl]oxy}phenyl]ethylidene]amine (132.8 mg, 0.5005 mmol), [RhCl(coe)₂]₂ (36.0 mg, 0.0502 mmol), and (*S*)-diisopropyl-(8,9,10,11,12,13,14,15-octahydro-3,5-dioxo-4-phosphacyclohepta[2,1-*a*;3,4-*a'*]dinaphthalen-4-yl)amine (42.5 mg, 0.100 mmol), the title compound was also obtained as a colorless oil in 57.3 mg (65% yield) and 90% ee.

(2*R*,3*R*)-1-(2,3-Dimethyl-2,3-dihydrobenzofuran-4-yl)ethanone ((2*R*,3*R*)-53) [Table 6, entry 8]

In a glovebox, to a medium-walled NMR tube was added a mixture of [RhCl(coe)₂]₂ (3.5 mg, 0.0049 mmol) and (*S*)-(8,9,10,11,12,13,14,15-octahydro-3,5-dioxo-4-phosphacyclohepta[2,1-*a*;3,4-*a'*]dinaphthalen-4-yl)-bis((*R*)-1-phenylethyl)amine (5.5 mg, 0.010 mmol) in 1,4-dioxane (0.40 mL) and a solution of benzyl-[1-{3-(1-methylpropenyloxy)phenyl}ethylidene]amine (*Z*/*E* = 4/1 for olefin) (13.9 mg, 0.0497 mmol) in 1,4-dioxane (0.10 mL). The tube was fitted with a Cajon adapter, the mixture was frozen, and then the tube was flame sealed under vacuum.

The NMR tube was then placed in oil bath heated to 50 °C for 72 h. After the reaction, the sealed tube was opened and the mixture was concentrated. To the residue was added 1,4-dioxane (0.50 mL) and concentrated HCl/H₂O (1/1) (0.50 mL). The mixture was stirred at room temperature for 3 h and then was extracted with diethyl ether four times. The combined organic layer was concentrated and the residue was purified by silica gel column chromatography (silica gel: 15 mL, eluted with 20:1 hexanes/ethyl acetate) to give the title compound as a colorless oil (5.6 mg, 59% yield). IR (ZnSe, thin film) ν_{\max} (cm⁻¹): 1680, 1583, 1442, 1355, 1263, 1231. ¹H NMR (400 MHz, CDCl₃): δ 7.38 (d, *J* = 8.0 Hz, 1H), 7.21 (t, *J* = 8.0 Hz, 1H), 6.96 (d, *J* = 8.0 Hz, 1H), 4.75 (quint, *J* = 6.8 Hz, 1H), 3.83 (quint, *J* = 6.8 Hz, 1H), 2.60 (s, 3H), 1.49 (d, *J* = 6.8 Hz, 3H), 1.06 (d, *J* = 6.8 Hz, 3H). ¹³C{¹H} NMR (100 MHz, CDCl₃): δ 199.0, 160.1, 135.4, 133.6, 128.0, 122.3, 114.0, 83.3, 40.0, 28.1, 15.0, 13.8. HRMS (EI): *m/z* calcd. for C₁₂H₁₄O₂ (M⁺): 190.0994, found: 190.0993. Chiral HPLC (Chiralcel AS column, 0.5% *i*PrOH/hexanes, 1mL/min): major, 13.5 min; minor, 12.7 min; 93% ee. CD (*c* = 4 × 10⁻⁵ M, MeOH): λ_{\max} ($\Delta\epsilon$): 251 (+6.20). A ¹H-¹H NOESY spectrum of (**2R,3R**)-**53** indicated that the geometry of the two protons on the dihydrofuran ring was *cis*.

Supplementary Material

Refer to Web version on PubMed Central for supplementary material.

Acknowledgements

This work was supported by NIH Grant GM069559 (to J.A.E.) and the Director and Office of Energy Research, Office of Basic Energy Sciences, Chemical Sciences Division, U.S. Department of Energy, under Contract DE-AC03-76SF00098 (to R.G.B.). Support for H.H. by Eisai Co., Ltd. is also gratefully acknowledged. We thank Dr. Frederick J. Hollander of the UC Berkeley CHEXray facility for solving the X-ray crystal structures of the *N*-sulfinyl imine (**S_SR**)-**33** and hydrazone (**2R,3R**)-**34** used to determine the absolute configurations of (**R**)-**19** and (**2R,3R**)-**30**, respectively.

References

- For recent reviews of C–H activation, see: (a) Alberico D, Scott ME, Lautens M. *Chem Rev* 2007;107:174–238. [PubMed: 17212475] (b) Godula K, Sames D. *Science* 2006;312:67–72. [PubMed: 16601184] (c) Kakiuchi F, Chatani N. *Top Organomet Chem* 2004;11:45–79. (d) Davies HML, Beckwith REJ. *Chem Rev* 2003;103:2861–2903. [PubMed: 12914484] (e) Ritleng V, Sirlin C, Pfeffer M. *Chem Rev* 2002;102:1731–1769. [PubMed: 11996548] (f) Jia C, Kitamura T, Fujiwara Y. *Acc Chem Res* 2001;34:633–639. [PubMed: 11513570] (g) Miura M, Satoh T. *Top Organomet Chem* 2005;14:55–83. (h) Campeau LC, Fagnou K. *Chem Soc Rev* 2007;37:1058–1068. [PubMed: 17576474]
- Murai S, Kakiuchi F, Sekine S, Tanaka Y, Kamatani A, Sonoda M, Chatani N. *Nature* 1993;366:529–531.
- (a) Jun C-H, Hong J-B, Kim Y-H, Chung K-Y. *Angew Chem Int Ed* 2000;39:3440–3442. (b) Lim SG, Ahn JA, Jun CH. *Org Lett* 2004;6:4687–4690. [PubMed: 15575661]
- (a) Thalji RK, Ahrendt KA, Bergman RG, Ellman JA. *J Am Chem Soc* 2001;123:9692–9693. [PubMed: 11572698] (b) Ahrendt KA, Bergman RG, Ellman JA. *Org Lett* 2003;5:1301–1303. [PubMed: 12688744] (c) Thalji RK, Ahrendt KA, Bergman RG, Ellman JA. *J Org Chem* 2005;70:6775–6781. [PubMed: 16095296]
- (a) O'Malley SJ, Tan KL, Watzke A, Bergman RG, Ellman JA. *J Am Chem Soc* 2005;127:13496–13497. [PubMed: 16190703] (b) Wilson RM, Thalji RK, Bergman RG, Ellman JA. *Org Lett* 2006;8:1745–1747. [PubMed: 16597156] (c) Watzke A, Wilson RM, O'Malley SJ, Bergman RG, Ellman JA. *Synlett* 2007:2383–2389.
- For a leading reference on enantioselective carbenoid and nitrenoid insertions see: Davies HML, Manning JR. *Nature* 2008;451:417–424. [PubMed: 18216847]
- Fujii N, Kakiuchi F, Yamada A, Chatani N, Murai S. *Chem Lett* 1997;26:425–426.

8. Kakiuchi F, Le Gendre P, Yamada A, Ohtaki H, Murai S. *Tetrahedron Asymmetry* 2000;11:2647–2651.
9. Han X, Widenhoefer RA. *Org Lett* 2006;8:3801–3804. [PubMed: 16898821]
10. (a) Taura Y, Tanaka M, Wu X-M, Funakoshi K, Sakai K. *Tetrahedron* 1991;47:4879–4888. (b) Barnhart RW, Wang X, Noheda P, Bergens SH, Whelan J, Bosnich B. *J Am Chem Soc* 1994;116:1821–1830. (d) Barnhart RW, McMorran DA, Bosnich B. *Chem Commun* 1997:589–590. For an innovative strategy for the intramolecular hydroacylation of alkynes for the catalytic asymmetric synthesis of cyclopentenones via kinetic resolution see: (e) Tanaka K, Fu GC. *J Am Chem Soc* 2002;124:10296–10297. [PubMed: 12197729] (f) Kundu K, McCullagh JV, Morehead AT Jr. *J Am Chem Soc* 2005;127:16042–16043. [PubMed: 16287288]
11. Shi BF, Maugele N, Zhang YH, Yu JQ. *Angew Chem Int Ed* 2008;47:EarlyView
12. Thalji RK, Bergman RG, Ellman JA. *J Am Chem Soc* 2004;126:7192–7193. [PubMed: 15186153]
13. (a) Arnold LA, Imbos R, Mandoli A, de Vries AHM, Naasz R, Feringa BL. *Tetrahedron* 2000;56:2865–2878. (b) Watanabe T, Knöpfel TF, Carreira EM. *Org Lett* 2003;5:4557–4558. [PubMed: 14627382] (c) Hua Z, Vassar VC, Choi H, Ojima I. *Proc Nat Acad Sci* 2004;101:5411–5416. [PubMed: 15020764] (d) Zhang FY, Chan ASC. *Tetrahedron Asymmetry* 1998;9:1179–1182. (e) Duursma A, Minnaard AJ, Feringa BL. *Tetrahedron* 2002;58:5773–5778. (f) Alexakis A, Burton J, Vastra J, Benheim C, Fournioux X, van den Heuvel A, Levêque J-M, Mazé F, Rosset S. *Eur J Org Chem* 2000:4011–4027.
14. van den Berg M, Minnaard AJ, Haak RM, Leeman M, Schudde EP, Meetsma A, Feringa BL, de Vries AHM, Malijaars CEP, Willans CE, Hyett D, Boogers JAF, Henderickx HJW, de Vries JG. *Adv Synth Catal* 2003;345(1 2):308–323.
15. (a) Fleming I, Henning R, Parker DC, Plaut HE, Sanderson PEJ. *J Chem Soc, Perkin Trans 1* 1995;4:317. (b) Fleming I. *Chemtracts: Org Chem* 1996;9:1.
16. Tamao K. *Adv Silicon Chem* 1996;3:1.
17. Feringa BL. *Acc Chem Res* 2000;33:346–353. [PubMed: 10891052]
18. Jun C-H, Moon CW, Hong J-B, Lim S-G, Chung K-Y, Kim Y-H. *Chem Eur J* 2002;8:485–492.

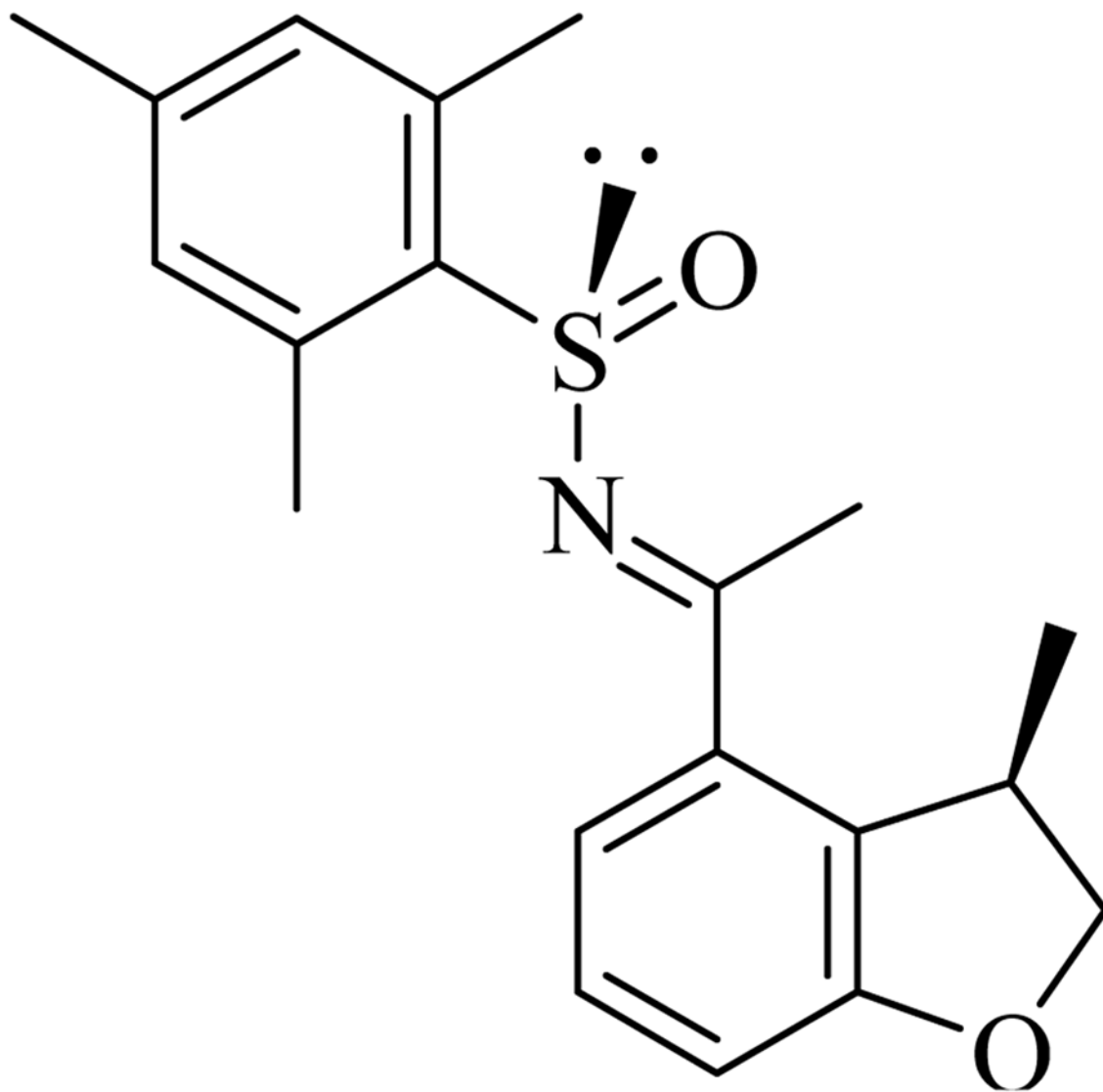


Figure 1.
Absolute configuration determined by X-ray structure obtained of sulfanyl imine (S,S,R)-33

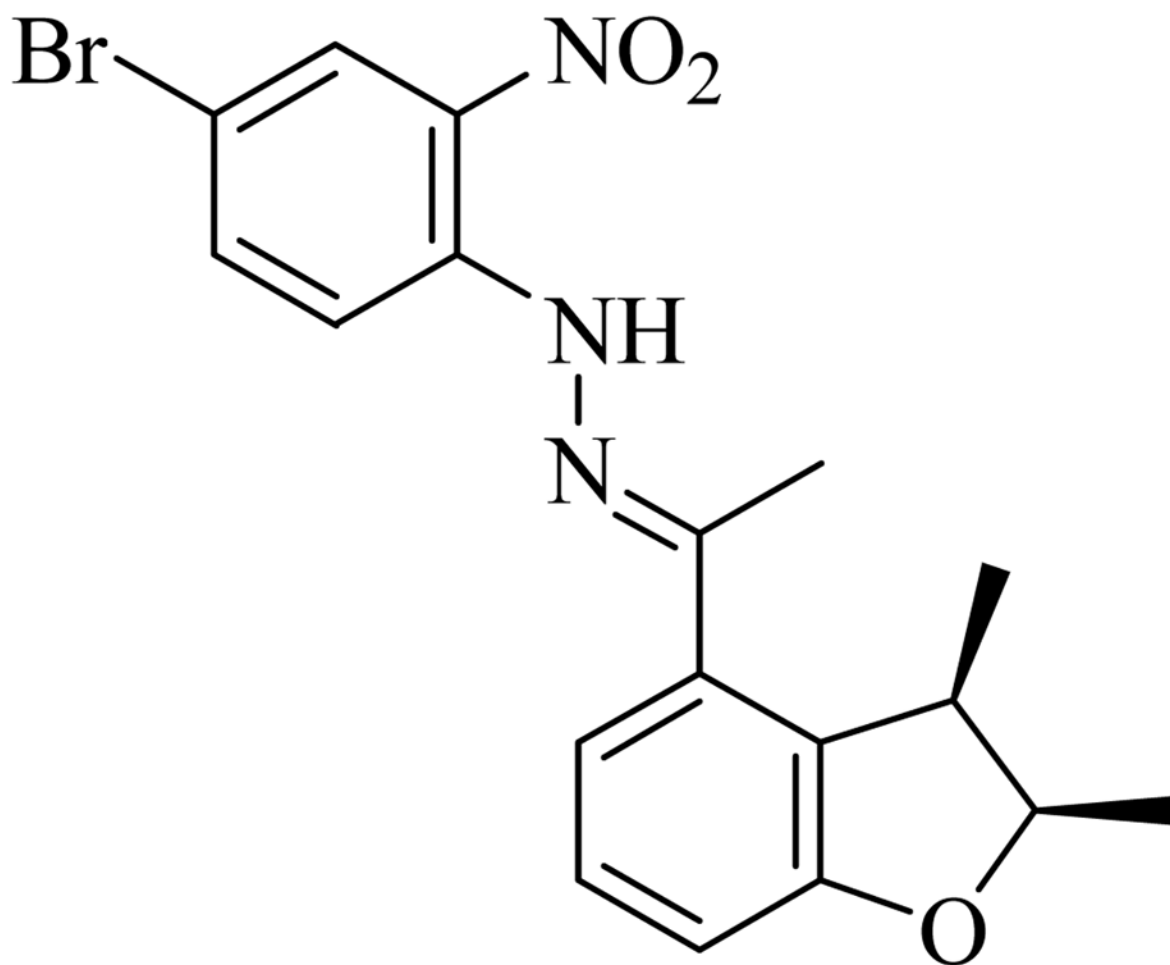
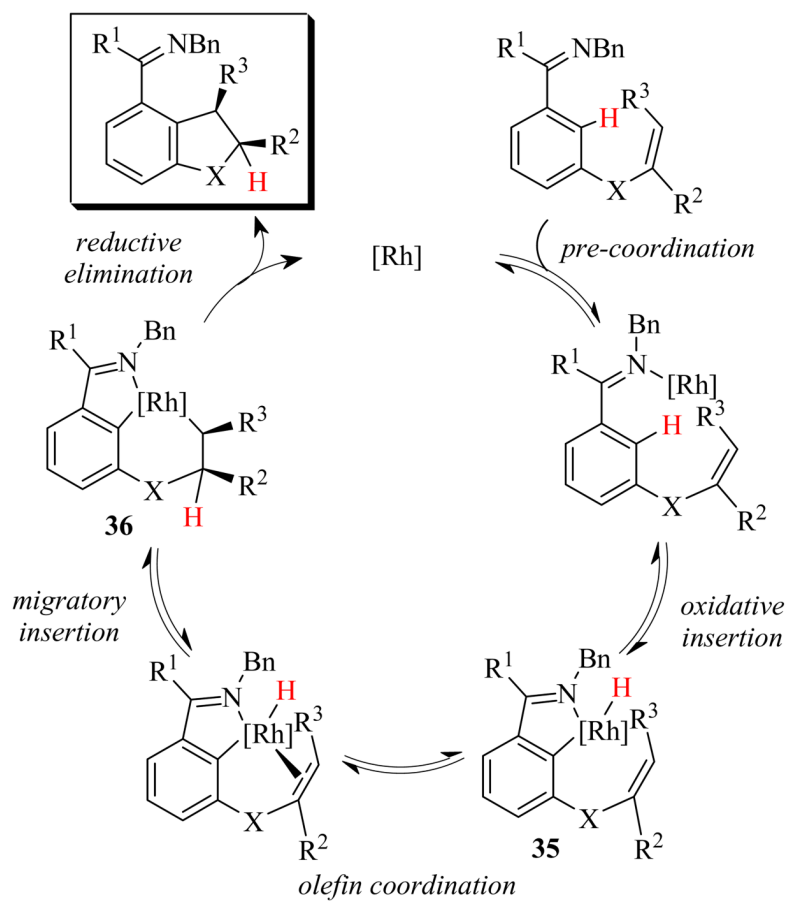
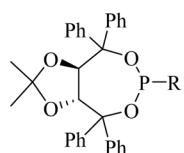


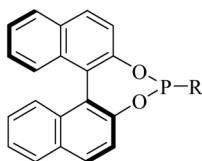
Figure 2. Absolute configuration determined by X-ray structure obtained hydrazone (*2R,3R*)-34

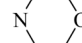


Scheme 1.

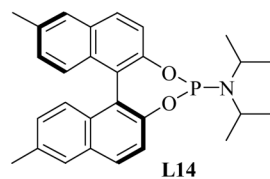


L1 : R = OMe
 L2 : R = OPh
 L3 : R = OMenthyl
 L4 : R = Ph

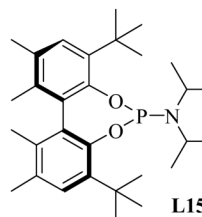


L5 : R = OPh
 L6 : R = NMe₂
 L7 : R = 
 L8 : R = NBn₂
 L9 : R = N(*i*-Pr)₂
 L10 : R = N((*R*)-(CHCH₃Ph))₂
 L11 : R = N((*S*)-(CHCH₃Ph))₂

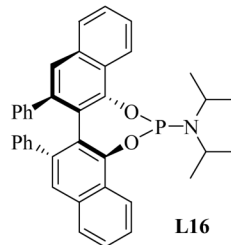
L12: R = N(*c*-C₆H₁₁)₂
 L13: R = N(*i*Pr)(*t*Bu)



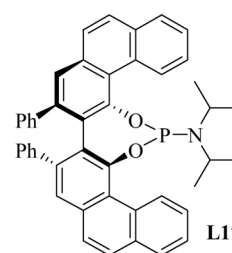
L14



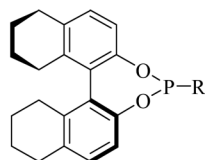
L15



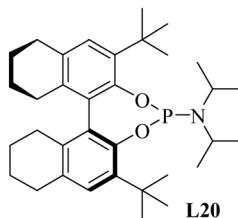
L16



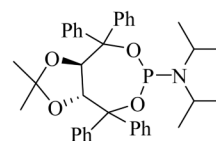
L17



L18: R = N(*i*Pr)₂
 L19: R = N((*R*)-(CHCH₃Ph))₂



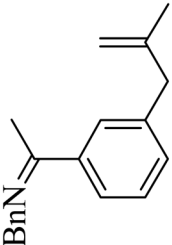
L20

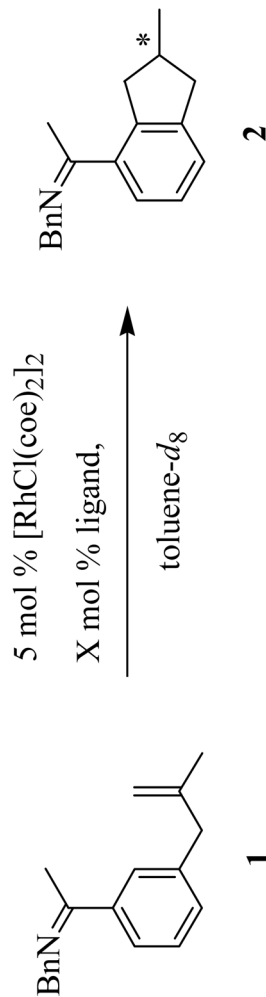


L21

Chart 1.
 Chiral Monodentate Phosphorus Ligands

Table 1
Asymmetric Cyclization of Alkene **1** Using Various Chiral Monophosphine Ligands

entry	ligand	ligand (mol%)	temp (°C)	time (h)	% yield ^d	% ee ^b
1		15	75	20	93 ^c	17 (R)
2	L2	15	75	20	94 ^c	9 (R)
3	L3	15	75	20	91 ^c	38 (R)
4	L4	15	125	20	34 ^c	0
5	L5	15	125	20	6 ^c	n.t.
6	L6	15	125	2.5	15 ^c	19 (S)
7	L7	15	125	2.5	14 ^c	0
8	L8	15	125	2.5	52 ^c	58 (S)
9	L9	5	125	1	96 ^d	83 (S)
10	L9	10	125	1	98 ^d	83 (S)
11	L9	15	125	<2	100	83 (S)
12	L9	20	125	6	0	--
13	L9	30	125	6	0	--
14	L10	15	125	<2	100	88 (S)
15	L11	15	125	<2	99	87 (S)



^aYields based on ¹H-NMR integration relative to 2,6-dimethoxytoluene internal standard.

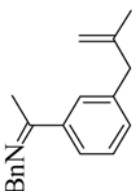
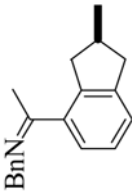
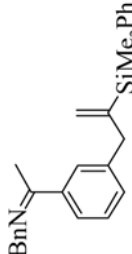
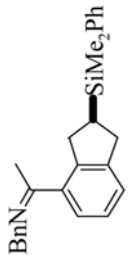
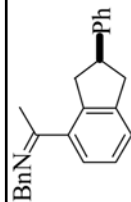
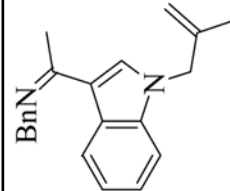
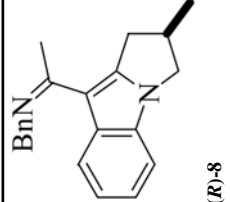
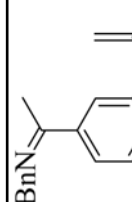
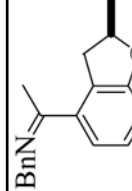
^bEe's determined after hydrolysis of **2** with 1N HCl (aq) using chiral GC or HPLC. Sense of induction is indicated in parentheses. n.t.: not tested.

^cRemainder of mass balance is unreacted starting material.

^dRemainder of mass balance is the double bond isomer of **1**.

Table 2

Asymmetric Cyclization of 1,1-Disubstituted Alkenes^{a,b}

substrate	product	Entry	ligand	temp (°C)	time (h)	% yield ^c	% ee ^d
 1	 (S)-2	1 ^e	L9	50	48	65 ^f	93
		2	L10	50	9	94	95
		3 ^e	L11	50	48	92	95
 3	 (S)-4	4	L9	125	0.3	91	70
		5	L10	50	20	75	25
		6	L11	125	0.25	100	27
		7	L11	50	20	96	42
 5	 (S)-6	8	L9	75	4	100	83
		9	L10	75	3	96	90
		10	L11	75	3.5	98	90
 7	 (R)-8	11 ^e	L9	125	12	78	63
		12 ^e	L10	125	1	90	70
		13 ^e	L11	125	1	99	68
 9	 (R)-10	14	L9	50	>200	69	89
		15	L10	50	1.5	99	93
		16	L10	rt	23	95	96
		17	L11	50	1.5	99	95
18	L11	rt	100	99	96		

^aReactions performed using 5 mol % [RhCl(cod)2]2 and 15 mol % ligand in toluene-48.

^bThe absolute configurations of (*S*)-**6** and (*R*)-**10** were assigned by chemical derivatization and X-ray structure determination (see reference ¹²). The absolute configurations of (*S*)-**2**, (*S*)-**4**, and (*R*)-**8** were assigned by analogy.

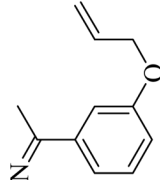
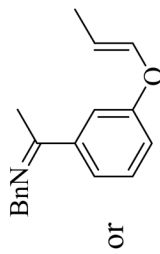
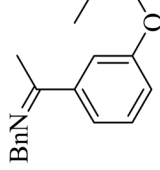
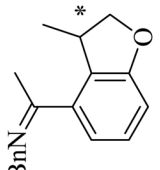
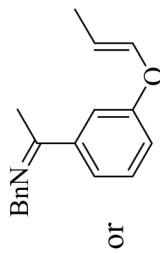
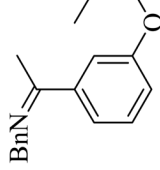
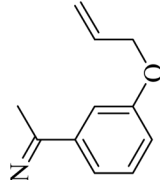
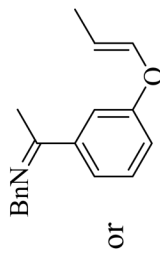
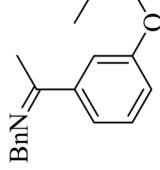
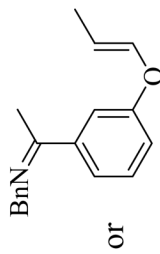
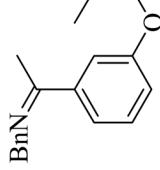
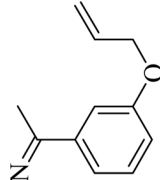
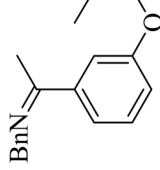
^cYields based on ¹H-NMR integration relative to 2,6-dimethoxytoluene internal standard.

^dEe's determined after hydrolysis of the imine product using chiral GC or HPLC.

^ePerformed using 10 mol% ligand.

^fYield is low due to unreacted material (9%) and formation of double bond isomer (20%).

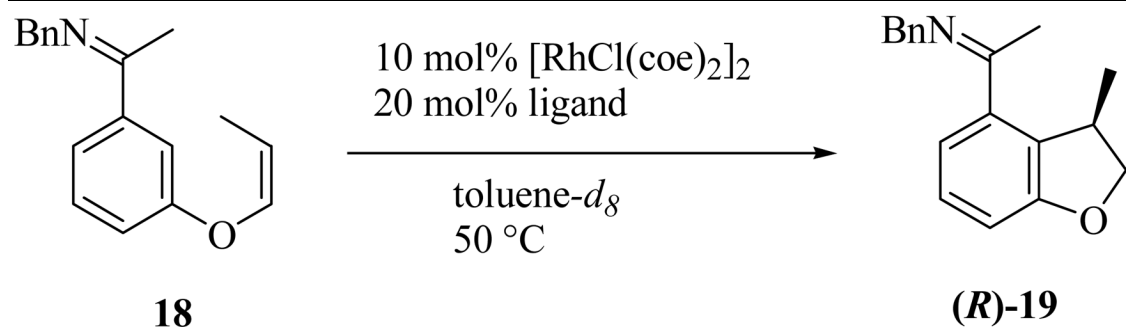
Table 3
Comparison of Isomeric Substrates for Asymmetric Cyclization

Entry	substrate	time (h)	17, % ^a	18, % ^a	%yield ^d	% ee ^b
1		96	--	--	19	< 22 (S) ^c
2		0	83	n.d.	n.d.	--
		6	53	25	6	--
		20	35	29	25	--
		44	26	24	39	--
		72	23	19	47	--
3		96	21	16	51	84 (R)
		0	n.d.	90	n.d.	--
		6	12	53	32	--
		21	10	24	57	--
		45	12	12	75	--
		74	10	7	80	--
		96	10	4	82	85 (R)

^a Amount of **17** and **18**, and yields based on ¹H NMR integration relative to 2,6-dimethoxytoluene internal standard. n.d.: not detected.

^b Ee's determined after hydrolysis of **19** with silica gel using chiral HPLC. Sense of induction is indicated in parentheses.

^c Approximate value due to peak overlapping in HPLC analysis.

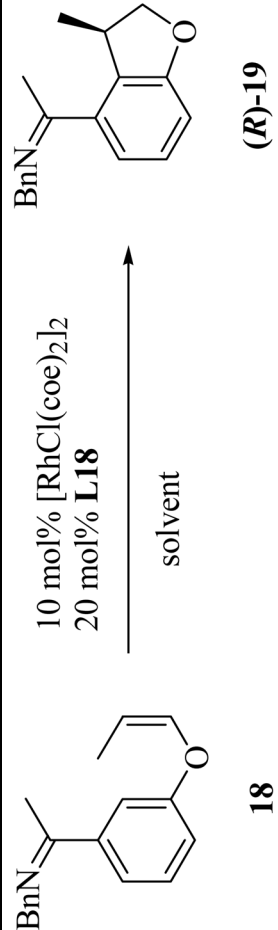
Table 4Asymmetric Cyclization of Alkene **18** Using Various Chiral Phosphoramidite Ligands

entry	ligand	time (h)	%yield ^a	% ee ^b
1	L8	44	7	n.t.
2	L9	20	44	--
		96	76	87
3	L10	45	75	--
		96	82	85
4	L11	96	61	85
5	L12	96	71	77
6	L13	20	2	n.t.
7	L14	96	64	90
8	L15	95	27	80
9	L16	21	81	86
10	L17	43	76	88
11	L18	96	82	91
12	L19	68	79	87
13	L20	96	20	78
14	L21	95	6	5

^aYields based on ¹H NMR integration relative to 2,6-dimethoxytoluene internal standard.

^bEe's determined after hydrolysis of (**R**)-**19** with silica gel using chiral HPLC. n.t.: not tested.

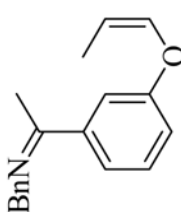
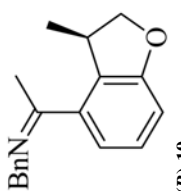
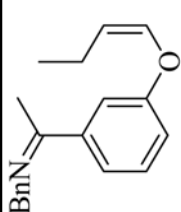
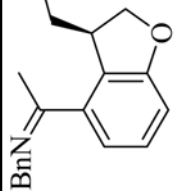
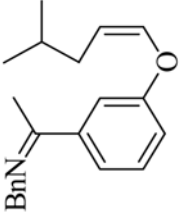
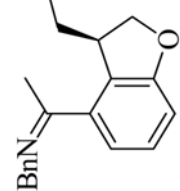
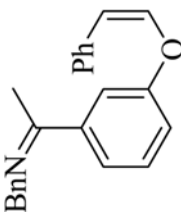
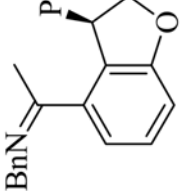
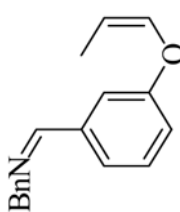
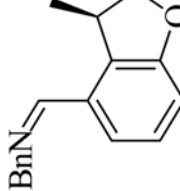
Table 5

Solvent Effects in Asymmetric Cyclization of Alkene **18**


entry	solvent	temp (°C)	time (h)	% yield ^a	% ee ^b
1	toluene- <i>d</i> ₆	50	45	65	--
2	toluene- <i>d</i> ₈	75	96	82	91
3	THF- <i>d</i> ₈	50	20	93	89
4	dioxane- <i>d</i> ₆	50	47	74	91
			46	82	90

^aYields based on ¹H NMR integration relative to 2,6-dimethoxytoluene internal standard.^bEe's determined after hydrolysis of (*R*)-**19** with silica gel using chiral HPLC.

Table 6
Asymmetric Cyclization of 1,2-Disubstituted and 1,1,2-Trisubstituted Alkenes^a

substrate	product	entry	ligand	temp (°C)	time (h)	%yield ^b	%ee ^c
		1	L18	50	46 (46–48) ^d	82 (65–71) ^e	90
18							
		2	L18	50	96	76 (53) ^e	91–92
20							
		3	L18	75	67	69 (48) ^e	90
22							
		4	L18	75	21 (22) ^d	93 (65) ^e	87
24							
		5 6 7	L16 L18 L19	75 75 75	72 96 72	53 25 40 (27) ^e	82 84 87–89
26							

substrate	product	entry	ligand	temp (°C)	time (h)	%yield ^b	% ee ^c
 29 (Z/E = 4/1)	 (2 <i>R</i> ,3 <i>R</i>)-30	8	L19	50	72	80 (59) ^e	91–93
 31 (Z/E = 9/1)	 (2 <i>S</i> ,3 <i>R</i>)-32	9 ^g	L19	75	92	50 (45) ^e	89–90

^aReactions performed using 10 mol % [RhCl(coe)₂]₂ and 20 mol % ligand in 1,4-dioxane-*d*₈ or 1,4-dioxane.

^bYield of *N*-benzylimine product determined by ¹H NMR using 2,6-dimethoxytoluene as an internal standard.

^cEe's determined after hydrolysis of products with silica gel or HCl/H₂O-dioxane using chiral HPLC.

^dFigures in parentheses are for the experiments for ketone product isolation.

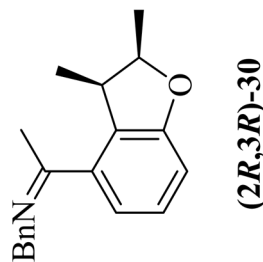
^eIsolated yield obtained after hydrolysis with HCl/H₂O-dioxane, which hydrolyzed not only the *N*-benzylimine but also any unreacted vinyl ether starting material.

^fReaction carried out in toluene-*d*₈. ^gIn the NMR-experiment, the reaction solution was heated at 50 °C for 6 h before increasing the temperature to 75 °C.

Table 7

Asymmetric Cyclization of Alkene **28** and **29**

entry	Substrate	Ligand	temp (°C)	solvent	time (h)	<i>E</i> -alkene (%)	<i>Z</i> -alkene (%)	%yield ^d	% ee ^b
1	28	L16	75	toluene- <i>d</i> ₈	0 6 20 47 68	84 55 41 33 31	n.d. n.d. 2 3 5	n.d. 21 32 38 40	-- -- -- -- 31
2	29 toluene- <i>d</i> ₈	L16 6 20	75 10 4		0 14 4	18 66 81	69 -- 69	n.d.	--
3	29 dioxane- <i>d</i> ₈	L16 6 22	50 15 13		0 10 n.d.	19 72 81	75 -- 80	n.d.	--
4	29 dioxane- <i>d</i> ₈	L18 6.5 22 46 72	50 16 16 14 13		0 45 20 7 2	17 30 60 69 74	70 -- -- -- 88	n.d.	--
5	29 dioxane- <i>d</i> ₈	L19 6 21 48 72	50 21 20 20 20		0 49 22 <10 ^c <7 ^c	21 29 59 74 80	78 -- -- -- 91	n.d.	--

**28: E-isomer****29: Z-rich mixture (Z/E = 4/1)****(2R,3R)-30**^a Amount of olefin isomers and yields based on ¹H NMR integration relative to 2,6-dimethoxytoluene internal standard. n.d.: not detected.^b *Ee*'s determined after hydrolysis of **(2R,3R)-30** with silica gel using chiral HPLC.^c Approximate value due to peak overlapping in ¹H NMR.